ACES Asian Chemical Editorial Society

doi.org/10.1002/asia.202401833

CHEMISTRY
AN ASIAN JOURNAL
Research Article

www.chemasianj.org

Non-Symmetrical Tetradentate Mixed Halogen Bonding-Hydrogen Bonding Macrocycles for Anion Recognition in Aqueous-Organic Media

Somjutar Opascharoenboon,[a] Sutthipoj Vigromsitdet,[a] Norraset Cheevathanomsak,[a] Inkarat Atirojwanich,[a] Jonggol Tantirungrotechai,[a] Mongkol Sukwattanasinitt,[b] Panida Surawatanawong,[a] Paul D. Beer,[c] and Thanthapatra Bunchuay*[a]

The prevalence of anions in biological systems, the environment, and industrial processes has driven the development of synthetic receptors capable of their selective recognition and detection. As a result of high hydration energy, the diversity in shape, and the pH-dependent nature of anions, such receptors require a highly preorganized binding site decorated with complementary multiple noncovalent interactions to stabilize anion-receptor complexation. In this study, a series of charge-neutral tetradentate macrocycles with non-symmetrical structures containing both halogen bonding (XB) iodotriazole and hydrogen bonding (HB) triazole donors were prepared via a stepwise CuAAC macrocyclization reaction. The non-symmetrical XB/HB macrocycles displayed increased anion binding affinities and contrasting anion selectivities in comparison to a symmetrical all HB macrocycle analogue, even in the presence of water, but still exhibited halide binding less strongly than the analogous all XB macrocycle. As a result of the macrocyclic effect and the number and nature of donor groups, the non-symmetrical XB/HB macrocycles exhibited the largest enhancement of Cl^- binding compared to their acyclic XB analogues. DFT computational studies revealed the preferential binding geometry where the halide anion was primarily bound to the XB binding site through two σ-hole interactions at two adjacent iodine sites and supplemented by one H—bond interaction at one of the C—H triazole sites.

1. Introduction

The versatility of anions in biological processes, industry, and the environment has continuously stimulated the development and synthesis of novel artificial anion receptors capable of functioning in aqueous media under physiological conditions.[1] Anions are crucial in biological systems, playing vital roles in the regulation of enzyme and protein functions; hence, anion receptors must exhibit robust interactions with excellent selectivity for the target anionic species. Malfunctions of anion receptors can lead to serious pathological conditions; for instance, dysregulation of the chloride membrane transport protein results in cystic fibrosis and is also linked to Alzheimer's disease,[2] while iodide is essential for the biosynthesis of tyrosine-based hormones by the thyroid gland.[3] The excessive use of phosphate and nitrate fertilizers has resulted in the eutrophication of natural water bodies and the disruption of ecosystems.[4]

In nature, biotic anion receptors, such as phosphate binding protein (PBP) and sulfate binding protein (SBP), employ a complementary arrangement of multiple hydrogen bonding noncovalent interactions within distinct hydrophobic binding pockets to overcome hydration enthalpies of highly hydrated phosphate and sulfate anions, leading to strong and selective binding of such oxoanions despite the presence of other interferences.[5] In recent decades, chemists have drawn inspiration from nature to create synthetic receptors for diverse anionic species, establishing anion recognition as a principal research focus in supramolecular host–guest chemistry.[6] Hydrogen bonding (HB) donor motifs have been integrated into a broad range of anion receptors that function in highly competitive solvent media.[7] Versatile NH bond donors, in particular, are represented in contemporary anion receptors in various forms, including ammonium, guanidinium, amide, urea, and thiourea.[6b,8] In more recent years, anion binding has been achieved utilizing preorganized C—H donors, especially as an alternative motif for the

[a] S. Opascharoenboon, S. Vigromsitdet, N. Cheevathanomsak, I. Atirojwanich, J. Tantirungrotechai, P. Surawatanawong, T. Bunchuay
Department of Chemistry and Center of Excellence for Innovation in Chemistry (PERCH-CIC), Faculty of Science, Mahidol University, Rama VI Rd, Thung Phayathai, Ratchathewi, Bangkok 10400, Thailand
E-mail: thanthapatra.bun@mahidol.edu
thanthapatra.bun@mahidol.ac.th

[b] M. Sukwattanasinitt
Department of Chemistry, Faculty of Science, Chulalongkorn University, Phyathai Road, Wangmai, Pathumwan, Bangkok 10330, Thailand

[c] P. D. Beer
Chemistry Research Laboratory, Department of Chemistry, University of Oxford, Mansfield Rd, Oxford OX1 3TA, UK

Somjutar Opascharoenboon and Sutthipoj Vigromsitdet contributed equally.

Supporting information for this article is available on the WWW under https://doi.org/10.1002/asia.202401833

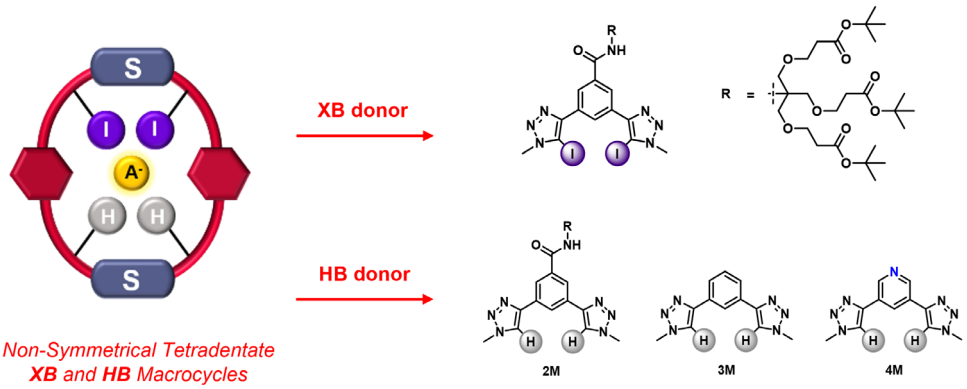

Figure 1. A cartoon represents a series of non-symmetrical tetradentate XB iodotriazole and HB triazole macrocycles.

binding of more hydrophobic anions.[9] The synthetic feasibility of the 1,2,3-triazole heterocycles through a copper(I) catalyzed alkyne-azide cycloaddition (CuAAC) reaction has allowed the facile accessibility to prepare a broad range of triazole rings with different electronic properties and made the C—H triazole HB donor become a potent candidate in anion recognition.[10] In addition, with iodoalkyne starting materials, the novel halogen bonding (XB) donor 5-iodo-1,2,3-triazole motif can be readily synthesized.[11] The high polarizability of the iodine atom with the stringent linear directionality of the XB interaction by virtue of the localized electropositive region (σ-hole) has facilitated the XB formation with various anionic Lewis bases.[12]

Beer and coworkers have utilized the iodotriazole and iodotriazolium XB donor motifs incorporated into preorganized host molecules with significant structural diversity, including acyclic, macrocyclic, and mechanically interlocked structures, to demonstrate enhanced anion binding, especially for halides, in aqueous environments compared to their HB host counterparts.[13] In addition, XB donor strength can be tuned to achieve augmented anion binding affinities by covalent modifications with electron-withdrawing groups and/or incorporation of positive charge component to the receptors.[13,14] Recently, Beer and Bunchuay designed a series of charge-neutral halogen-bonding macrocycles containing a tetradentate-iodotriazole binding site separated by different spacer units (*meta*-xylyl, *para*-xylyl, and naphthyl).[15] The size of the aryl spacer units was shown to strongly influence anion binding affinity through macrocyclic cavity size variation, as evidenced by halide binding affinities of the regio-isomeric xylyl-substituted macrocycles and the *meta*-xylyl substituted macrocycle displaying remarkable halide binding in highly competitive 40% aqueous-organic D_2O/d_6-acetone (40:60, v/v) solvent mixtures.

In this study, through the construction of a series of charge-neutral non-symmetrical mixed XB/HB and all XB and HB tetradentate triazole macrocycles, we investigate the effect of the XB and HB triazole donor groups on anion recognition in pure organic and water-containing organic solvents. The non-symmetrical XB/HB tetradentate triazole macrocycles containing the 3,5-bis-iodotriazole benzene XB donor supplemented with various bis-triazole HB donors were synthesized via stepwise sequential CuAAC macrocyclization reactions (Figure 1). Subsequently, the anion recognition properties of each macrocycle were examined through ^{1}H-NMR spectroscopic titrations, and the results were compared to those of acyclic receptors and the symmetrical all XB and HB tetradentate triazole macrocycles. Notably, the symmetrical HB macrocycle displayed significantly lower halide binding affinities in comparison to the XB analogue and showed favorable binding to Cl^- despite the presence of water. The presence of XB donors in the series of non-symmetrical macrocycles significantly improved halide binding affinities and modulated selectivity toward larger halide anions Br^- and I^-. Importantly, analysis of the anion binding data of the bis-iodotriazole pyridine mixed XB/HB macrocycle revealed a 7-, 5-, and 2-fold increase in the association constants for Cl^-, Br^- and I^-, respectively, in comparison to an acyclic XB receptor analogue. DFT computational investigations revealed the most favorable halide anion-macrocycle complexed structures, with the estimated binding energies consistent with experimental results.

2. Results and Discussion

2.1. Synthesis of Acyclic Receptors

Having demonstrated that the strength of XB donors is highly sensitive to covalent functionalization with electron-withdrawing groups,[13,16] we sought to explore the effect of electron-deficient aromatic units in the 1,3-bis-iodotriazole anion receptors on their anion binding properties. We initially synthesized a series of 1,3-bis-iodotriazole XB acyclic receptors from the copper(I) catalyzed azide-alkyne cycloaddition (CuAAC) reaction. An excess of 1,3-bis(azidomethyl) benzene **2** was reacted with one equivalent of the selected bis-iodoalkyne in the presence of a catalytic amount CuI and TBTA, affording the target XB receptors containing the phenyl spacer (**1·XB**), the phenyl-substituted with amide spacer (**2·XB**), and the pyridyl spacer (**3·XB**) with an isolated yield in the range of 70%–80% (Scheme 1). In addition, the HB analogous receptors (**1·HB**, **2·HB**, and **3·HB**) were also synthesized for comparisons. All products were fully characterized by ^{1}H-NMR, ^{13}C-NMR, and HRMS to confirm the structure of receptors.

Comparative ^{1}H-NMR spectra of the XB acyclic receptors revealed that the chemical shifts of the internal aromatic proton (H_a), proton associated with the anion binding site, are

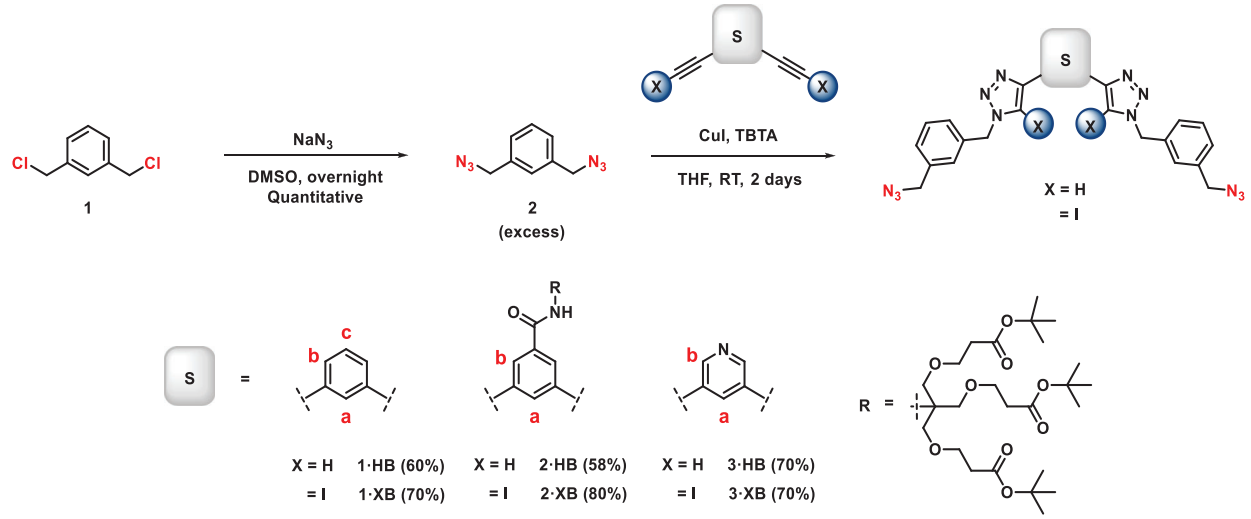

Scheme 1. Synthesis of XB and HB acyclic receptors containing different arene spacer units via the CuAAC reaction.

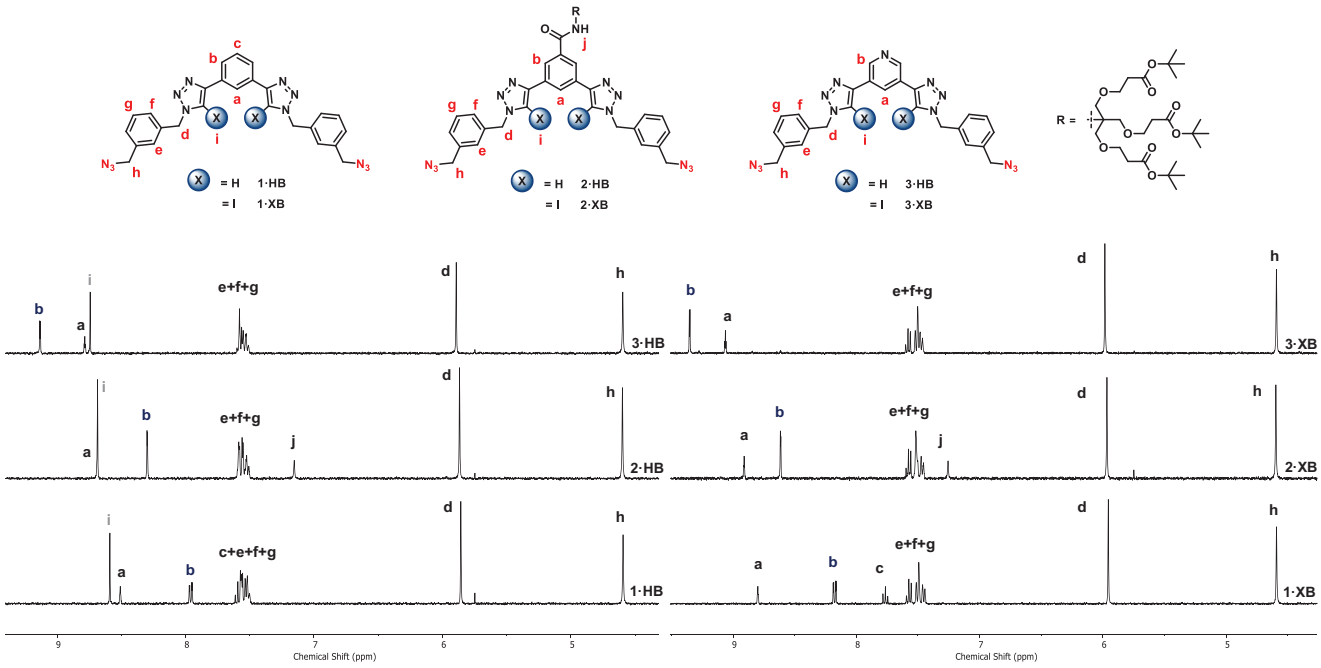

Figure 2. Stacking of truncated ^{1}H-NMR spectra of XB and HB acyclic receptors (d_6-acetone, 298 K, 400 MHz).

significantly influenced by the local electronic characteristics of the aromatic spacer groups originating from the bis-alkyne (Figure 2). When compared to **1·XB**, the chemical shift of H_a in **2·XB**, and **3·XB** is located in further downfield regions as a result of the electron-withdrawing effect from the amide and pyridyl groups, respectively. These similar effects were also observed in HB analogues. In addition, the iodine substituent in the bis-iodotriazole motifs of XB receptors also induced downfield perturbations of proton signals encircling the binding site (H_a and H_d). These evidences proved the potency of utilizing covalent modification to incorporate electron-drawing groups to the receptors for modulating electronic properties of the anion binding site.

2.2. Synthesis of Macrocyclic Receptors

Given the findings of our earlier report,[11] the stepwise macrocyclization methodology based on the CuAAC reaction not only improves the effectiveness of macrocyclization reaction, but also allows for the synthesis of a series of non-symmetrical macrocycles including mixed XB and HB ditopic binding sites.[8a,15,17] The bis-azide appended HB acyclic receptors (**1·HB**, **2·HB**, and **3·HB**) are reactive precursors for the macrocyclization reaction undertaken by reacting with an equimolar amount of the bis-iodoalkyne **3** in the presence of $Cu(MeCN)_4PF_6$ and TBTA in a dilute solution (5 mM in DCM). The reactions gave the target non-symmetrical macrocyclic products **2M**, **3M**, and **4M** with

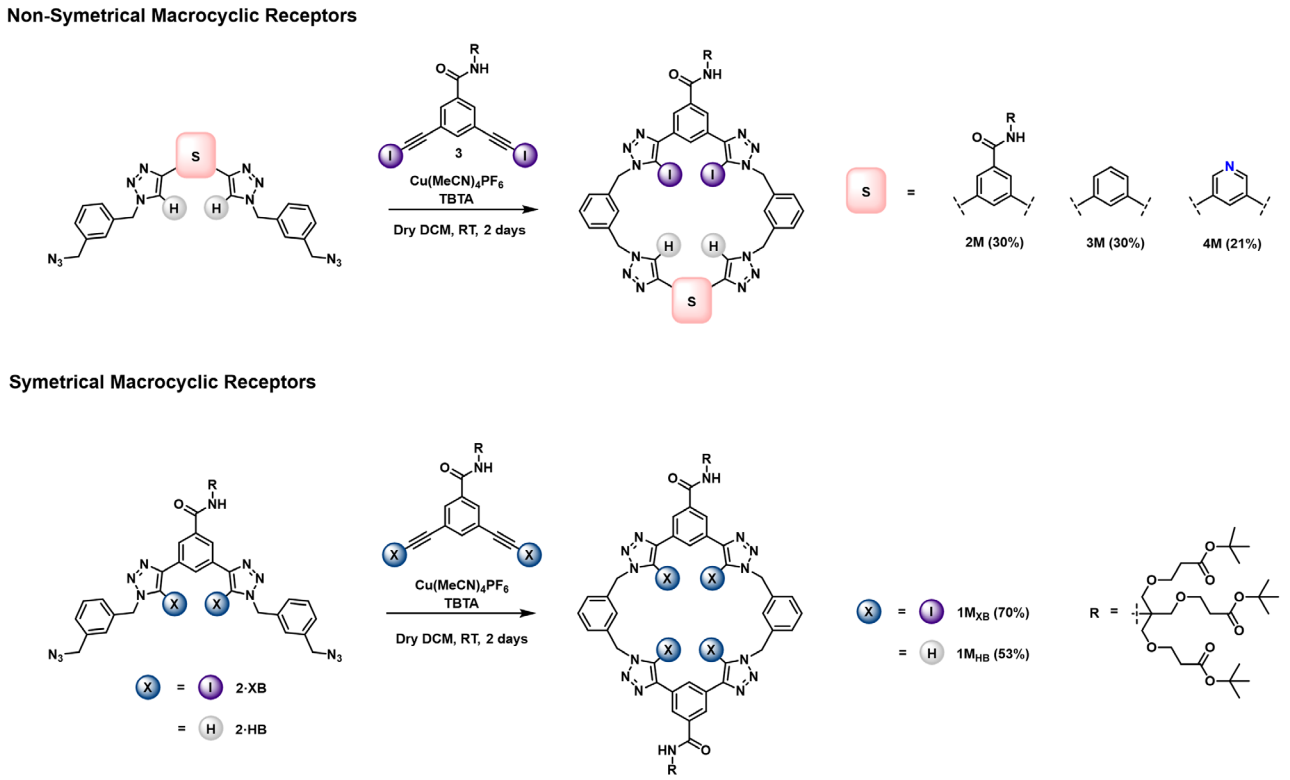

Scheme 2. Synthesis of macrocyclic receptors (**1M$_{XB}$**, **1M$_{HB}$**, **2M**, **3M**, and **4M**) containing the HB or XB donors and different arene spacer units.

isolated yields of 30%, 30%, and 21%, respectively (Scheme 2). Similar to the cases of both HB and XB acyclic receptors, the electronic characteristics of the aromatic spacer groups influenced the chemical shift of H_a and H_m in the ^{1}H-NMR spectra of **2M**, **3M**, and **4M** (Figure 3). For comparative anion binding studies, the tetradentate triazole all XB and HB macrocycles **1M$_{HB}$** and **1M$_{XB}$** were also synthesized.[15]

2.3. Anion Binding Studies

2.3.1. Anion Binding in D_6-Acetone

The halide anion recognition properties of acyclic XB receptors (**1·XB**, **2·XB**, and **3·XB**) and their respective HB analogues (**1·HB**, **2·HB**, and **3·HB**) were initially studied in the d_6-acetone via ^{1}H-NMR anion titration experiments. Upon addition of chloride, bromide, and iodide, as their tetrabutylammonium (TBA) salts to solutions of the acyclic receptors, significant downfield perturbations of the internal aromatic proton (H_a) signal, the proton signal associated with the anion binding cleft, were observed. Furthermore, HB receptors exhibited notable shifts of triazole protons (H_i) to downfield regions (Figure S25–S48). By monitoring the shifts of H_a in the acyclic XB and HB receptors as a function of anion concentrations, binding isotherms were obtained, which from the nonlinear regression analysis via Bindfit,[18] determined 1:1 stoichiometric host–guest association constants (Table 1). The acyclic HB receptors bound halides weakly in d_6-acetone and displayed an anion binding trend mirroring anion basicity ($Cl^- > Br^- > I^-$). Importantly, the analogous acyclic XB receptors demonstrated significantly augmented halide binding affinities of approximately up to two-orders of magnitude enhancement compared to HB analogues, particularly for the **2·XB** and **3·XB** receptors, which contain the amide and pyridyl electron-withdrawing units, respectively.

The incorporation of **2·HB** into the macrocyclic scaffold produced the tetradentate HB triazole macrocycle **1M$_{HB}$**. The determined K_a values in d_6-acetone for Cl^- (4601 M^{-1}), Br^- (2991 M^{-1}), and I^- (296 M^{-1}) correspond to a 50-, 75-, and 99-fold respective enhancement of halide association constants in comparison to acyclic analogue **2·HB**, even though they exhibit the same halide binding trend (Table 1). These results indicate that integration of the bis-triazole **2·HB** into the macrocyclic scaffold results in significantly augmented binding affinities for all halides by virtue of the macrocyclic effect and double the number of preorganized polarized triazole C—H bonds. Importantly, **1M$_{HB}$** and Flood's triazolophane share a common characteristic, since both macrocycles comprise four units of HB triazole groups for anion binding. In acetone, **1M$_{HB}$** demonstrated approximately two-order of magnitude lower K_a value for Cl^- binding. This considerable difference can be elucidated by the size-complementarity of the anion binding cavity and chloride. The aromatic electron-withdrawing groups directly attached to the triazole unit in Flood's triazolophane enhance the polarization of the triazole binding unit, making it a potent hydrogen bond donor,[19] whereas the methylene link in **1M$_{HB}$** diminishes this effect. It is noteworthy to mention that the acyclic XB analogue **2·XB** demonstrated superior halide binding affinities to

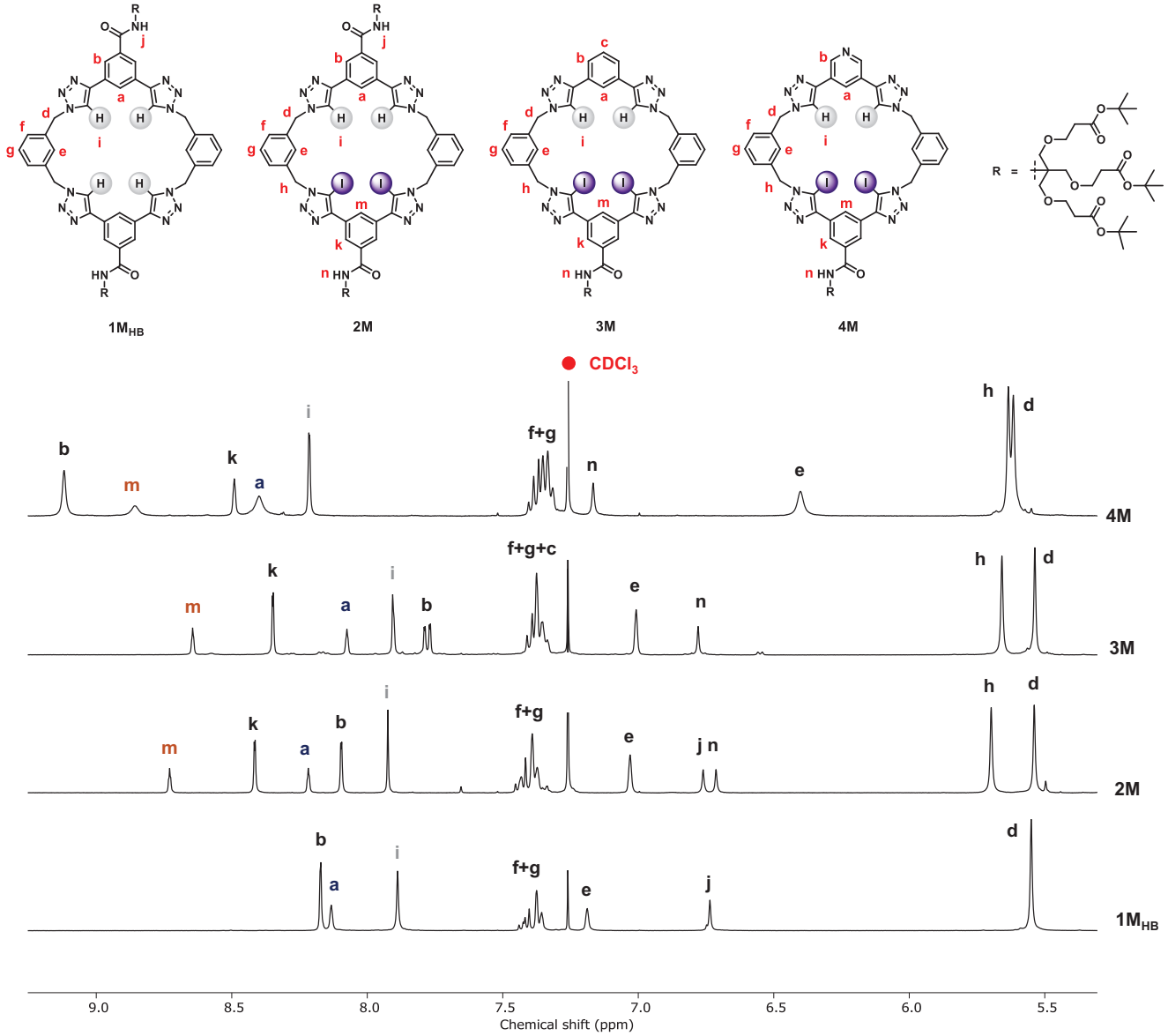

Figure 3. Stacking of truncated ^{1}H-NMR spectra of **1M$_{HB}$, 2M, 3M,** and **4M** macrocyclic receptor ($CDCl_3$, 298 K, 400 MHz).

Table 1. Halide anion association constants (K_a, M^{-1}) of XB and HB acyclic receptors (1 mM) with tetrabutylammonium halide salts titration in d_6-acetone at 298 K, % error exhibited in parenthesis.

Anion	Association Constants (K_a, M^{-1}) in d_6-Acetone										
	Phenyl Spacer		Amide Spacer		Pyridyl Spacer		Macrocycles				
	1·HB	1·XB	2·HB	2·XB	3·HB	3·XB	1M$_{XB}$	1M$_{HB}$	2M	3M	4M
Cl^-	77 (1)	5075 (3)	92 (1)	7684 (4)	72 (1)	$>10^4$	$>10^4$	4601 (6)	$>10^4$	$>10^4$	$>10^4$
Br^-	48 (1)	3087 (2)	40 (2)	4382 (4)	66 (1)	$>10^4$	$>10^4$	2991 (3)	$>10^4$	5799 (5)	$>10^4$
I^-	9 (2)	1193 (1)	3 (1)	1256 (2)	7 (2)	3450 (1)	$>10^4$	296 (1)	3027 (5)	2157 (1)	4747 (13)

the HB macrocycle **1M$_{HB}$**. Not surprisingly, **1M$_{XB}$**, the tetradentate all XB iodotriazole macrocyclic analogue of **2·XB**, exhibited the highest affinities with K_a values $>10^4$ M^{-1} for all halides. The integration of both HB triazole and XB iodotriazole donor groups into a macrocyclic scaffold produces the mixed XB/HB non-symmetrical macrocycle **2M** that has separate bidentate XB and HB binding sites. Additions of TBA halide salts to a solution of **2M** induced chemical shift changes of proton signals encircling the binding site including the internal aromatic protons (H_a and H_m), the triazole protons (H_i), and the xylyl proton (H_e) to downfield

perturbations (Figure S53–S55). Additionally, other proton signals derived from the *m*-xylyl spacer unit (H_f and H_g) shift to upfield region, suggesting a conformational change of **2M** upon anion coordination. Bindfit analysis of chemical shift as a function of anion concentration determined 1:1 stoichiometric host-guest association constants of **2M**, where the receptor exhibited $K_a > 10^4$ M^{-1} for Cl^- and Br^- complexation and $K_a = 3027$ M^{-1} for I^-. In the case of **3M**, the trend of K_a values follows the anion basicity while **4M** exhibited K_a values for Cl^- and Br^- $>10^4$ M^{-1} and for I^- of 4747 M^{-1}. The results highlighted the fact that incorporations of the pyridyl electron-withdrawing substituent could enhance anion binding properties of the non-symmetrical XB/HB macrocyclic receptors as obviously observed in the case of iodide binding (Table 1).

2.3.2. Anion Binding in 5% D_2O/D_6-Acetone

The presence of water in polar organic media typically results in diminished anion binding affinities, and this effect is highly pronounced, especially for highly hydrated anions.[8a,20] Our attention subsequently turned to investigate the halide binding affinities of both the acyclic and macrocyclic receptors in the more competitive solvent mixture, 5% v/v D_2O/d_6-acetone, via analogous ^{1}H-NMR titration experiments. As expected, all the acyclic XB receptors revealed substantial attenuations in halide binding affinities and switching of halide selectivity to the preferential complexation of binding the larger halides, reflecting the Hofmeister bias trend K_a: $I^- > Br^- > Cl^-$.[21] Indeed, the determined K_a values of XB acyclic receptors for iodide binding (in the range of 273–371 M^{-1}) are comparable to the K_a value derived from the tetradentate XB iodotriazole [2]rotaxane ($K_a = 562$ M^{-1}).[20] Under the same titration conditions, with all halides, negligible perturbations of the proton signals in HB acyclic receptors were noted, indicating no binding in the wet organic solvent.

Halide binding studies in 5% v/v D_2O/d_6-acetone were also carried out with the macrocyclic receptors. The chemical shift changes of the internal aromatic proton (H_a) upon anion complexation were monitored, and binding isotherms analyzed via BindFit determined the 1:1 stoichiometric host–guest association constants. The tetradentate triazole HB receptor $\mathbf{1M}_{HB}$ exhibited downfield perturbation of proton signals encircling the binding site in the presence of TBABr (0–10 equiv), where $\Delta\delta$ of triazole-proton (H_i), aromatic-proton arene spacer (H_a), and amide-proton dendrimer (H_c) = 0.7, 0.3, and 0.07 ppm, respectively. Despite titrations carried out in the media containing water $\mathbf{1M}_{HB}$ displayed chloride binding with $K_a = 182$ M^{-1}, comparable to bromide ($K_a = 132$ M^{-1}) and bound iodide weakly ($K_a = 44$ M^{-1}) notably following the anti-Hofmeister binding trend, whereas the HB acyclic analogue **2·HB** did not bind halides. The XB analogue $\mathbf{1M}_{XB}$, the reference macrocyclic receptor, exhibited anion association constants with $K_a > 10^5$ M^{-1} for all halides in 5% v/v D_2O/d_6-acetone, suggesting that the tetradentate XB donors are potent and capable of enhancing halide binding affinities in aqueous media.

According to the binding properties of $\mathbf{1M}_{HB}$ and $\mathbf{1M}_{XB}$, it was quite intriguing to see the effect of using macrocycles containing both HB and XB binding sites within the same molecules for anion binding studies. Upon additions of anion solutions to the non-symmetrical mixed XB-HB macrocycle **2M,** proton signals surrounding the binding cavity including an internal aromatic proton of the XB site (H_m), an internal aromatic proton of the HB site (H_a), triazole protons (H_i), aromatic spacer protons (H_e) display notable downfield shifts (Figure 4). In addition, both H_f and H_g display notable upfield shifts upon anion complexations as a result of the shielding effect and conformational changes of the macrocycle. In addition, the degree of signal perturbations from the XB and HB binding sites are similar (Figure S81–S83), implying anion complexations occurred at the central cavity between both bidentate binding sites. The convergence of proton signals (H_d) and (H_h) indicated macrocycle conformation changes induced by anion bindings. Bindfit analysis of 1:1 host–guest stoichiometric binding isotherms determined association constants derived from **2M** in which the receptor showed the highest binding affinity for Br^- with $K_a = 328$ M^{-1} followed by I^- ($K_a = 232$ M^{-1}) and Cl^- ($K_a = 39$ M^{-1}), whereas **2·XB** showed the highest K_a value for I^- with $K_a = 273$ M^{-1} followed by Br^- ($K_a = 72$ M^{-1}) and Cl^- ($K_a = 26$ M^{-1}). Importantly, the results indicate the possibility of tuning halide anion binding selectivity by adjusting the electronic and steric properties of the binding site, as well as strategically combining XB/HB donors within a host structural framework. Even though the non-symmetrical XB/HB macrocycles exhibit lower K_a values for halide bindings compared to the symmetrical XB macrocyclic analogue $\mathbf{1M}_{XB}$, the results indicated that the non-symmetrical XB/HB macrocycles can be employed for the selective recognition of various anions, hence enhancing the diversity of complexation interactions. For instance, **2M** exhibited enhanced binding affinity for Br^- compared to a significantly hydrated Cl^- and a highly polarized I^-. Replacing the aromatic spacer of the HB donor site in **2M** with benzene and pyridyl produced **3M** and **4M**, respectively. The pyridyl substituted receptor **4M** displayed notable downfield shifts of triazole protons (H_i) with $\Delta\delta = 0.45$ ppm in the presence of 0–10 equiv TBABr (Figure S90, Table S19), while such proton in **2M** and **3M** showed a smaller $\Delta\delta = 0.40$ and 0.37, respectively (Figure S82 and S86, Table S19). Not surprisingly, **4M** formed the relatively strongest halide complexes among the non-symmetrical XB/HB macrocyclic receptors displaying the Hofmeister selectivity trend (Table 2). The superior halide binding of **4M** highlighted the effect of the pyridyl electron-withdrawing group on the enhancement of anion recognition in aqueous media. Impressively, **4M** displayed a 7-, 5-, and 2-fold enhancement for Cl^-, Br^-, and I^- association constants compared to **2·XB**, an acyclic XB analogue.

2.4. Computational Study

2.4.1. Density Functional Calculations (DFT)

Density functional calculation was performed in order to gain insights into the electronic structures related to the binding of chloride to symmetrical XB and non-symmetrical HB-XB receptors (Figure 5). We calculated the truncated structures of the XB macrocycle $\mathbf{1M}_{XB}$ and the non-symmetrical macrocycle

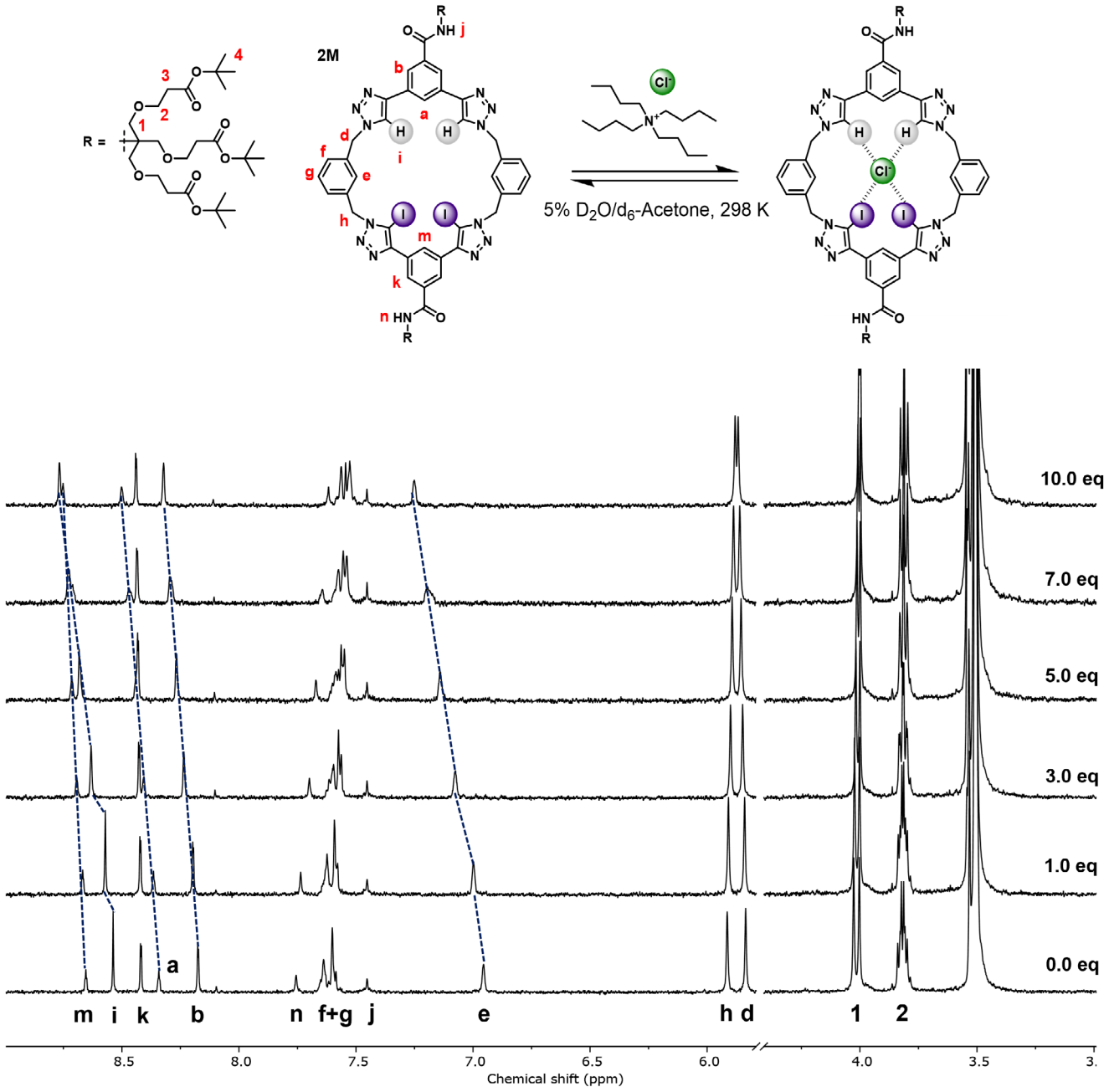

Figure 4. Stacking of ^{1}H-NMR spectra of macrocyclic receptor **2M** in 5% v/v D_2O/d_6-acetone (298 K, 400 MHz) in the presence of TBA chloride (0–10 equiv).

Table 2. Halide anion association constants (K_a, M^{-1}) of XB and HB acyclic receptors (1 mM) with tetrabutylammonium halide salts titration in 5% v/v D_2O/d_6-acetone at 298 K, % error exhibited in parenthesis.

Anion	Association Constants (K_a, M^{-1}) in 5% v/v D_2O/d_6-Acetone							
	Acyclic Receptors			Macrocyclic Receptors				
	1·XB	2·XB	3·XB	$1M_{XB}$[15]	$1M_{HB}$	2M	3M	4M
Cl^-	75 (3)	26 (12)	68 (1)	$>10^5$	182 (1)	39 (1)	116 (2)	177 (2)
Br^-	360 (1)	72 (4)	251 (2)	$>10^5$	132 (2)	328 (3)	145 (2)	367 (2)
I^-	371 (4)	273 (2)	350 (1)	$>10^5$	44 (1)	232 (1)	294 (4)	618 (3)

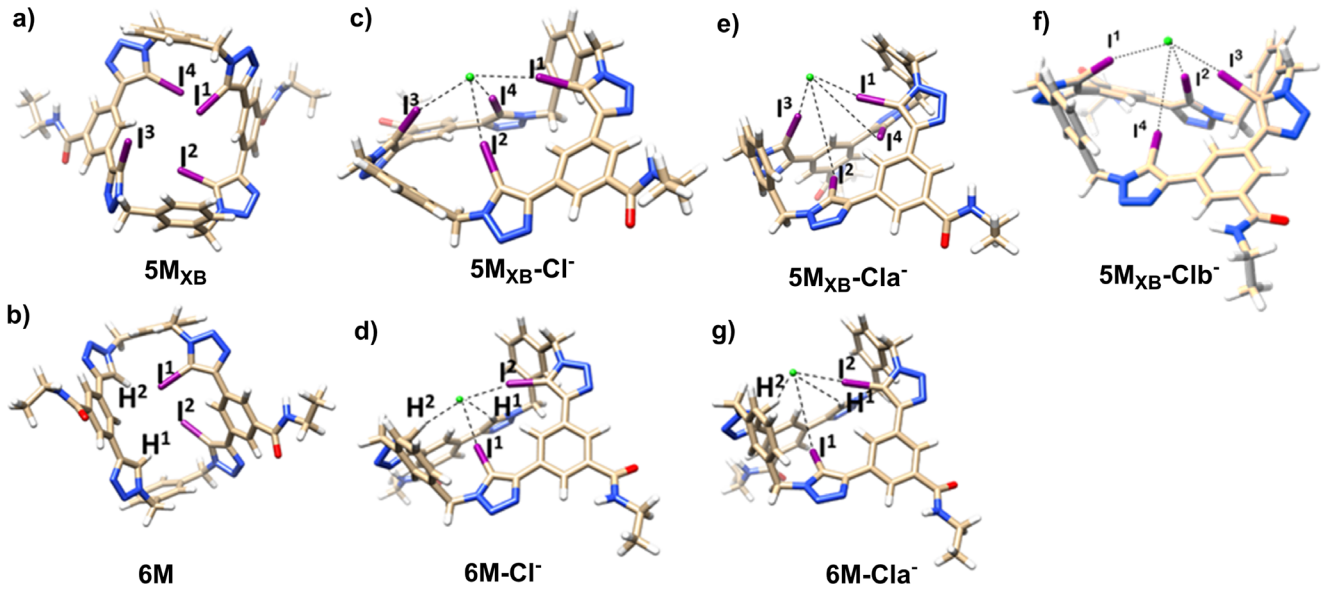

Figure 5. Optimized structure of a) **5M$_{XB}$**, b) **6M**, c) **5M$_{XB}$-Cl$^-$**, d) **6M-Cl$^-$**, e) **5M$_{XB}$-Cla$^-$**, f) **5M-Clb$^-$**, and g) **6M-Cla$^-$**.

Table 3. Solvent-corrected relative free energies in water for the binding of chloride to the XB and HB receptors.

Reactions	ΔG (kJ/mol)
5M$_{XB}$ + $[Cl(H_2O)_4]^-$ → **5M$_{XB}$-Cl$^-$** + $(H_2O)_4$	−56.0
5M$_{XB}$ + $[Cl(H_2O)_4]^-$ → **5M$_{XB}$-Cla$^-$** + $(H_2O)_4$	−22.7
5M$_{XB}$ + $[Cl(H_2O)_4]^-$ → **5M$_{XB}$-Clb$^-$** + $(H_2O)_4$	−55.9
6M + $[Cl(H_2O)_4]^-$ → **6M-Cl$^-$** + $(H_2O)_4$	−19.2
6M + $[Cl(H_2O)_4]^-$ → **6M-Cla$^-$** + $(H_2O)_4$	−16.6

2M with ethyl group on the amide substituents, that is, **5M$_{XB}$** and **6M**, respectively. The optimal conformations for initial structures were obtained from CREST conformational search.[22] The initial position of chloride was assigned at the center of the macrocycle **5M$_{XB}$** with distances between chloride and iodides approximately 2.9–3.1 Å based on the previously related crystal structures.[23] The lowest energy structure and selected structures with distinct chloride to C—I interactions from CREST were further optimized using DFT for **5M$_{XB}$-Cl$^-$**. The halide-water clusters[24] $[Cl(H_2O)_4]^-$ were considered for the calculation of the binding energy of chloride in water.

For **5M$_{XB}$**, three possible binding modes of chloride were considered. The binding energy of chloride to all four C—I bonds (**5M$_{XB}$-Cl$^-$**) (−56.0 kJ/mol) is comparable to the binding of chloride to three C—I bonds (**5M$_{XB}$-Clb$^-$**) (−55.9 kJ/mol); these two modes are more favorable than the binding of chloride to two opposite C—I bonds (**5M$_{XB}$-Cla$^-$**) (−22.7 kJ/mol) (Figure 5 and Table 3). In **5M$_{XB}$-Cl$^-$** with all four σ-hole interactions, the C—I···Cl distances are 3.1–3.2 Å (Figure S95). In **5M$_{XB}$-Clb$^-$**, there are only three σ-hole interactions with the C—I···Cl distances of 3.1 Å (Figure S95). According to the second-order perturbation energy, $\Delta E^{(2)}$, from natural bond orbital (NBO) analysis, the electron donation from the lone pair orbital (LP) of chloride (Cl^-) to the σ^* orbital of the receptor (C—I) was found (Table 4). The $\Delta E^{(2)}$ for the LP(Cl^-) donation to σ^*(C—I) is related to the extent of the σ-hole interaction.[15,25] Here, the chloride σ-hole receptors for XB are at all four C—I sites for **5M$_{XB}$-Cl$^-$**; the $\Delta E^{(2)}$ values for the LP(Cl^-) donation to all four σ^*(C—I) are similar (33.9–38.6 kJ/mol) (Table 4). For **5M$_{XB}$-Clb$^-$**, among the chloride interactions with three C—I sites, the LP(Cl^-) donation to two σ^*(C-I) ($\Delta E^{(2)}$ = 52.2 and 53.8 kJ/mol) are slightly stronger than the other σ^*(C—I) ($\Delta E^{(2)}$ = 47.1 kJ/mol) (Table 4). These suggest that chloride binds to all four σ-holes at the iodine sites in **5M$_{XB}$-Cl$^-$** while chloride binding to three σ-holes at the iodine sites in **5M$_{XB}$-Clb$^-$** cannot be disregarded.

For **6M**, two possible binding modes were obtained. The chloride binding to C—I^1 and C—I^2, located at the adjacent sites (**6M-Cl$^-$**) (−19.2 kJ/mol), was found slightly more favorable than the chloride binding to C—I^2 and C—H^2 located at the opposite sites (**6M-Cla$^-$**) (−16.6 kJ/mol) (Figure 5 and Table 3). In **6M-Cl$^-$**, in addition to two σ-hole interactions with two C-I···Cl distances of 3.0–3.1 Å, one H-bond interaction was found with C—H···Cl distance of 2.427 Å (Figure S96). These interactions correspond with the second-order perturbation energy, $\Delta E^{(2)}$. The $\Delta E^{(2)}$ values for the LP(Cl^-) donation to σ^*(C—I^1) and the LP(Cl^-) donation to σ^*(C—I^2) are 49.7 and 53.1 kJ/mol, respectively, while the $\Delta E^{(2)}$ for the LP(Cl^-) donation to σ^*(C—H^2) is 32.8 kJ/mol. This suggests the chloride binding with two σ-hole interactions at two adjacent iodine sites and one HB interaction at one of the C—H sites in **6M-Cl$^-$**.

Overall, the binding of chloride to **5M$_{XB}$** to form **5M$_{XB}$-Cl$^-$** (−56.0 kJ/mol) is more favorable than the binding of chloride to **6M** to form **6M-Cl$^-$** (−19.2 kJ/mol) (Table 3). This showed that the chloride ion binds to **5M$_{XB}$** stronger than to **6M**, which is in good agreement with the chloride association constant (K_a) for **1M$_{XB}$** and **2M** (>10^5 and 39 M^{-1}, respectively) (Table 2).

Table 4. Second-order perturbation energy, $\Delta E^{(2)}$, (in kJ/mol) for the orbital interactions from the lone pair of chloride, LP(Cl^-), to σ^*(C–I) and σ^*(C–H) of $5M_{XB}$ and **6M**.

Donor	Acceptor	$5M_{XB}$-Cl^-	$5M_{XB}$-Cla^-	$5M_{XB}$-Clb^-	6M-Cl^-	6M-Cla^-
LP (Cl^-)	σ^*(C-I^1)	38.6	86.9	47.1	49.7	–
LP (Cl^-)	σ^*(C-I^2)	37.7	–	53.8	53.1	107.6
LP (Cl^-)	σ^*(C-I^3)	33.9	72.7	52.2	–	–
LP (Cl^-)	σ^*(C-I^4)	38.1	–	–	–	–
LP (Cl^-)	σ^*(C-H^1)	–	–	-	9.5	–
LP (Cl^-)	σ^*(C-H^2)	–	–	–	32.8	39.5

3. Conclusion

In summary, non-symmetrical tetradentate macrocycles featuring mixed halogen bonding (XB) iodotriazole and hydrogen bonding (HB) triazole donor groups were successfully synthesized via sequential CuAAC-mediated macrocyclization. These macrocycles displayed significant enhancements in anion binding affinities, particularly for halides, when compared to a symmetrical all HB macrocycle or acyclic analogues, but bound halides less strongly than the previously-reported all-XB system. The presence of both XB and HB donors within a macrocyclic framework allowed for synergistic interactions that amplified binding strengths, especially for chloride, while maintaining adaptability across different anion targets. In aqueous-organic media, the binding affinities were attenuated due to anion hydration and competition from water molecules, with the effect more pronounced for smaller, highly hydrated anions such as chloride. Nonetheless, the mixed XB/HB macrocycles retained notable binding capabilities, particularly for larger halides like bromide and iodide, aligning with Hofmeister bias trends. Computational studies further revealed that halides were stabilized within the binding cavity by a combination of two σ-hole XB interactions at adjacent iodine sites and one HB interaction at a triazole C—H donor, emphasizing the role of donor diversity in overcoming water's disruptive effects. These findings highlight the potential of mixed XB/HB macrocycles as versatile and robust anion receptors, capable of selective recognition in challenging environments. Their tunable binding properties facilitate the design of advanced anion recognition systems, with future research focusing on enhancing performance in water-rich conditions through structural modifications, such as hydrophobic shielding or optimized cavity design.

Supporting Information

The authors have cited additional references within the Supporting Information (PDF).[8a,15,26]

Acknowledgements

This research is supported by the Office of the Permanent Secretary, Ministry of Higher Education, Science, Research and Innovation (Grant No. RGNS 65 -150) and funded by the National Research Council of Thailand (NRCT, N42A661000). T. B., J. T., P. S. and S. V. thank the Center of Excellence for Innovation in Chemistry (PERCH-CIC), Ministry of Higher Education, Science, Research and Innovation for financial support.

Conflict of Interests

The authors declare no conflict of interest.

Data Availability Statement

The data that support the findings of this study are available in the supplementary material of this article.

Keywords: Anion · Halogen bonding · Hydrogen bonding · Macrocycles · Supramolecular chemistry

[1] a) P. D. Beer, P. A. Gale, *Angew. Chem. Int. Ed.* **2001**, *40*, 486–516; b) P. A. Gale, E. N. W. Howe, X. Wu, *Chem* **2016**, *1*, 351–422.
[2] M. Rowe Steven, S. Miller, J. Sorscher Eric, *N. Engl. J. Med. 352*, 1992–2001.
[3] F. Delange, *Thyroid®* **1994**, *4*, 107–128.
[4] P. J. A. Withers, C. Neal, H. P. Jarvie, D. G. Doody, *Sustainability* **2014**, *6*, 5853–5875.
[5] a) F. Wolfe-Simon, J. S. Blum, T. R. Kulp, G. W. Gordon, S. E. Hoeft, J. Pett-Ridge, J. F. Stolz, S. M. Webb, P. K. Weber, P. C. W. Davies, A. D. Anbar, R. S. Oremland, *Science* **2011**, *332*, 1163–1166; b) T. J. Erb, P. Kiefer, B. Hattendorf, D. Günther, J. A. Vorholt, *Science* **2012**, *337*, 467–470; c) J. W. Pflugrath, F. A. Quiocho, *Nature* **1985**, *314*, 257–260; d) H. Luecke, F. A. Quiocho, *Nature* **1990**, *347*, 402–406.
[6] a) L. Chen, S. N. Berry, X. Wu, E. N. W. Howe, P. A. Gale, *Chem* **2020**, *6*, 61–141; b) M. J. Langton, C. J. Serpell, P. D. Beer, *Angew. Chem. Int. Ed.* **2016**, *55*, 1974–1987; c) D. A. McNaughton, W. G. Ryder, A. M. Gilchrist, P. Wang, M. Fares, X. Wu, P. A. Gale, *Chem* **2023**, *9*, 3045–3112; d) F. A. Mohammed, T. Xiao, L. Wang, R. B. P. Elmes, *Chem. Commun.* **2024**, *60*, 11812–11836.
[7] a) V. López-Corbalán, A. Fuertes, A. L. Llamas-Saiz, M. Amorín, J. R. Granja, *Nat. Commun.* **2024**, *15*, 6055; b) L. Jing, E. Deplazes, J. K. Clegg, X. Wu, *Nat. Chem.* **2024**, *16*, 335–342.
[8] a) N. G. White, S. Carvalho, V. Félix, P. D. Beer, *Org. Biomol. Chem.* **2012**, *10*, 6951–6959; b) N. A. Tzioumis, D. A. Cullen, K. A. Jolliffe, N. G. White, *Angew. Chem. Int. Ed.* **2023**, *62*, e202218360; c) S. M. Butler, M. Hountondji, S. N. Berry, J. Tan, L. Macia, K. A. Jolliffe, *Org. Biomol. Chem.* **2023**, *21*, 8548–8553.
[9] V. Haridas, S. Sahu, P. P. Praveen Kumar, A. R. Sapala, *RSC. Adv.* **2012**, *2*, 12594–12605.
[10] a) B. Qiao, A. Sengupta, Y. Liu, K. P. McDonald, M. Pink, J. R. Anderson, K. Raghavachari, A. H. Flood, *J. Am. Chem. Soc.* **2015**, *137*, 9746–9757; b) F. C. Parks, E. G. Sheetz, S. R. Stutsman, A. Lutolli, S. Debnath, K. Raghavachari, A. H. Flood, *J. Am. Chem. Soc.* **2022**, *144*, 1274–1287.

[11] a) W. S. Brotherton, R. J. Clark, L. Zhu, *J. Org. Chem.* **2012**, *77*, 6443–6455; b) J. E. Hein, J. C. Tripp, L. B. Krasnova, K. B. Sharpless, V. V. Fokin, *Angew. Chem. Int. Ed.* **2009**, *48*, 8018–8021.
[12] a) S. W. Robinson, C. L. Mustoe, N. G. White, A. Brown, A. L. Thompson, P. Kennepohl, P. D. Beer, *J. Am. Chem. Soc.* **2015**, *137*, 499–507; b) D. Mungalpara, S. Stegmüller, S. Kubik, *Chem. Commun.* **2017**, *53*, 5095–5098; c) K. Hengphasatporn, P. Wilasluck, P. Deetanya, K. Wangkanont, W. Chavasiri, P. Visitchanakun, A. Leelahavanichkul, W. Paunrat, S. Boonyasuppayakorn, T. Rungrotmongkol, S. Hannongbua, Y. Shigeta, *J. Chem. Inf. Model.* **2022**, *62*, 1498–1509.
[13] T. Bunchuay, A. Docker, A. J. Martinez-Martinez, P. D. Beer, *Angew. Chem. Int. Ed.* **2019**, *58*, 13823–13827.
[14] A. Docker, C. H. Guthrie, H. Kuhn, P. D. Beer, *Angew. Chem. Int. Ed.* **2021**, *60*, 21973–21978.
[15] T. Bunchuay, K. Boonpalit, A. Docker, A. Ruengsuk, J. Tantirungrotechai, M. Sukwattanasinitt, P. Surawatanawong, P. D. Beer, *Chem. Commun.* **2021**, *57*, 11976–11979.
[16] a) T. Bunchuay, T. Khianjinda, P. Srisawat, Y. C. Tse, C. Gateley, P. D. Beer, *Chem. Commun.* **2023**, *59*, 13615–13618; b) T. Bunchuay, A. Docker, U. Eiamprasert, P. Surawatanawong, A. Brown, P. D. Beer, *Angew. Chem. Int. Ed.* **2020**, *59*, 12007–12012.
[17] T. Zhao, V. M. Lynch, J. L. Sessler, *Org. Biomol. Chem.* **2022**, *20*, 980–983.
[18] BindFit v0.5 | Supramolecular, can be found under http://app.supramolecular.org/bindfit/.
[19] Y. Liu, A. Sengupta, K. Raghavachari, A. H. Flood, *Chem*, **2017**, *3*, 411–427.
[20] J. Y. C. Lim, T. Bunchuay, P. D. Beer, *Chem. Eur. J.* **2017**, *23*, 4700–4707.
[21] F. Hofmeister, *Arch. Exp. Path. Pharm.* **1888**, *24*, 247–260.
[22] a) P. Pracht, S. Grimme, C. Bannwarth, F. Bohle, S. Ehlert, G. Feldmann, J. Gorges, M. Müller, T. Neudecker, C. Plett, S. Spicher, P. Steinbach, P. A. Wesołowski, F. Zeller, *J. Chem. Phys.* **2024**, *160*, 114110; b) P. Pracht, F. Bohle, S. Grimme, *Phys. Chem. Chem. Phys.* **2020**, *22*, 7169–7192; c) S. Spicher, M. Bursch, S. Grimme, *J. Phys. Chem. C* **2020**, *124*, 27529–27541.
[23] B. R. Mullaney, A. L. Thompson, P. D. Beer, *Angew. Chem. Int. Ed.* **2014**, *53*, 11458–11462.
[24] G. Lamoureux, B. Roux, *J. Phys. Chem. B* **2006**, *110*, 3308–3322.
[25] a) S. M. Huber, E. Jimenez-Izal, J. M. Ugalde, I. Infante, *Chem. Commun.* **2012**, *48*, 7708–7710; b) B. Nepal, S. Scheiner, *J. Phys. Chem. A* **2015**, *119*, 13064–13073.
[26] a) C. M. Cardona, R. E. Gawley, *J. Org. Chem.* **2002**, *67*, 1411–1413; b) H. Dai, S. Yu, W. Cheng, Z.-F. Xu, C.-Y. Li, *Chem. Commun.* **2017**, *53*, 6417–6420; c) S. W. Robinson, P. D. Beer, *Org. Biomol. Chem.* **2017**, *15*, 153–159; d) M. J. Frisch, G. W. Trucks, H. B. Schlegel, G. E. Scuseria, M. A. Robb, J. R. Cheeseman, G. Scalmani, V. Barone, B. Mennucci, G. A. Petersson, H. Nakatsuji, M. Caricato, X. Li, H. P. Hratchian, A. F. Izmaylov, J. Bloino, G. Zheng, J. L. Sonnenberg, M. Hada, M. Ehara, K. Toyota, R. Fukuda, J. Hasegawa, M. Ishida, T. Nakajima, Y. Honda, O. Kitao, H. Nakai, T. Vreven, J. J. A. Montgomery, et al., *Gaussian 09* **2009**, *Revision B.01*. e) Y. Zhao, D. G. Truhlar, *Theor. Chem. Acc.* **2008**, *120*, 215–241; f) F. Weigend, R. Ahlrichs, *Phys. Chem. Chem. Phys.* **2005**, *7*, 3297–3305; g) P. C. Hariharan, J. A. Pople, *Theor. Chim. Acta.* **1973**, *28*, 213–222; h) G. A. Petersson, M. A. Al-Laham, *J. Chem. Phys.* **1991**, *94*, 6081–6090; i) G. A. Petersson, A. Bennett, T. G. Tensfeldt, M. A. Al-Laham, W. A. Shirley, J. Mantzaris, *J. Chem. Phys.* **1988**, *89*, 2193–2218; j) A. V. Marenich, C. J. Cramer, D. G. Truhlar, *J. Phys. Chem. B* **2009**, *113*, 6378–6396; k) G. Luchini, J. Alegre-Requena, I. Funes-Ardoiz, R. Paton, *F1000Research* **2020**, *9*, 291; l) T. Lu, F. Chen, *J. Comput. Chem.* **2012**, *33*, 580–592; m) E. D. Glendening, C. R. Landis, F. Weinhold, *J. Comput. Chem.* **2013**, *34*, 1429–1437; n) P. Ramírez-López, M. C. de la Torre, H. E. Montenegro, M. Asenjo, M. A. Sierra, *Org. Lett.* **2008**, *10*, 3555–3558; o) A. Borissov, J. Y. C. Lim, A. Brown, K. E. Christensen, A. L. Thompson, M. D. Smith, P. D. Beer, *Chem. Commun.* **2017**, *53*, 2483–2486.

Manuscript received: December 10, 2024
Revised manuscript received: April 14, 2025
Version of record online: ■■, ■■